Heliyon 9 (2023) e16682

Contents lists available at ScienceDirect

Heliyon

journal homepage: www.cell.com/heliyon

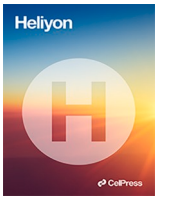

Triterpenoids of *Ganoderma lucidum* inhibited S180 sarcoma and H22 hepatoma in mice by regulating gut microbiota

Jiajia Wang, Junfeng Pu, Zhixian Zhang, Zean Feng, Jing Han, Xiaojie Su, Lei Shi *

Department of Pharmacy, Gansu Provincial Hospital, Lanzhou, Gansu, 730000, China

ARTICLE INFO

Keywords:
Triterpenoids
Ganoderma lucidum
Antitumor
Gut microbiota

ABSTRACT

In order to explore effect of natural plant extracts on anti-tumor and prevent tumor development. The study assessed the antitumor effect of triterpenoids of *Ganoderma lucidum* (TGL) on S180 and H22 tumor bearing mice. A triterpene compound, 2α, 3α, 23-trihydroxy-urs-12-en-28-oic acid, was successfully isolated and purified from *G. lucidum*. S180 and H22 cells were subcutaneously inoculated in the left axilla of mice to establish a transplantable tumor model. After, the mice were orally treated with TGL and evaluated by tumor inhibition rate, organ index, and the serum index. The Bax and Bcl-2 proteins and gut microbiota was analyzed using western blot and 16S rDNA sequencing respectively. The results showed the tumor inhibition rates of TGL were higher than 40% in H22 and S180 tumor bearing mice. TGL had a protective effect on the spleen and thymus, and improved lipid peroxidation caused by the increased free radicals. TGL down-regulated Bcl-2 and upregulated Bax. In particular, TGL treatment improved the reduction of gut microbiota richness and structure.

1. Introduction

Cancer is the second deadliest disease in the world after cardiovascular disease. The current chemotherapy used for the treatment of cancer is expensive and has serious side effects on healthy tissues [1]. The toxicity of chemotherapeutic drugs is still the main limitation of cancer treatment, and drug combinations have been widely applied for the treatment of cancer. The use of natural extracts as a potential adjunct therapy may reduce the toxicity of drug interactions, and potential synergies can reduce the resistance and possible toxicity of chemical drugs. Moreover, many substances with possible anti-tumor effects have been obtained from natural products such as plants and algae, which have attracted research attention [2]. In addition to ganoderma lucidum polysaccharides, triterpenoids *Ganoderma Lucidum* (TGL) are also its main active substances. The chemical structure of TGL is relatively complex, the relative molecular weight is generally between 400 and 600, and it is highly fat-soluble and difficult to dissolve in water. The triterpenoid compounds isolated from Ganoderma lucidum are mostly highly oxidizing lanostane derivatives with ganoderma lucidum acid as the main component, most of which are polar molecules with weak volatility. Clinical studies have shown that TGL have important effects in anti-tumor, anti-bacterial, anti-lipid, anti-inflammatory, immune regulation, improving memory and delaying aging [3,4]. Previous studies have shown that lentinan, schizophyllan, and polysaccharide-K can inhibit the growth of all sorts of transplantable tumors in experimental animals [5]. Yin et al. used triterpenoids from fruits of Sorbus pohuashanensis to improve the antioxidant effect and antitumor activity *in vivo* experiments [6].

* Corresponding author. Department of Pharmacy, Gansu Provincial Hospital, Donggang West Road No. 204, Lanzhou, Gansu 730000, China.
E-mail address: shilei2020_2020@163.com (L. Shi).

https://doi.org/10.1016/j.heliyon.2023.e16682
Received 12 November 2022; Received in revised form 20 May 2023; Accepted 24 May 2023
Available online 7 June 2023

Oxidative stress ensues when an imbalance occurs between active oxygen generation and removal [7]. Oxidative stress caused by reactive oxygen species (ROS) may be related to many human diseases, such as tumors. ROS induced structural breaks between single and double strands of nDNA or cross-links between DNA strands through oxidation, or caused changes in purines, pyrimidines, and deoxyribose to trigger nDNA mutations, leading to the activation of proto-oncogenes or the inactivation of tumor suppressor genes [8]. This genetic change caused abnormal cell proliferation to form tumors [8]. Antioxidants play an important role in guarding our bodies from various types of oxidative damage related to cancer [7]. Superoxide dismutase (SOD), malondialdehyde (MDA), and catalase (CAT) are important antioxidants which provide significant antioxidant defense [9]. In patients with solid tumors, an immunosuppressive microenvironment exists around tumor tissues which can prevent immune cells from exerting anti-tumor effects [10]. The spleen plays an pivotal role in the body's immune response as a peripheral lymphoid organ [11]. The thymus is a crucial source of cellular immunity and protects the body by providing a suitable microenvironment for the differentiation and maturation of T lymphocytes [12]. The thymus and spleen indices can reflect the immune status of the human body and immunotoxicity of anti-tumor drugs [13]. The pro-apoptotic protein Bax can inactivate anti-apoptotic proteins such as Bcl-2 [14]. Bcl-2 family proteins (including Bcl-2, Bax, etc.) play important roles in apoptosis and are considered to be the first regulatory step in inducing intrinsic mitochondrial apoptosis [15].

The changes in the composition of gut microbiota are related to local and systemic changes that affect tumor/cancer growth, in part by mucosal immunity, regulating tissue remodeling and anti-tumor immunity [16,17]. It has been studied that the gut microbial ecosystem can control intestinal immune homeostasis and inflammation and immune regulation of secondary lymphoid organs, eventually forming a tumor microenvironment [18]. Previous studies have found obvious immune suppression in tumor-bearing animals [19].

In order to explore the anti-tumor effect of natural extracts based on the gut microbiota, we used the therapeutic effect of TGL to treat mice with sarcoma S180 cells and hepatoma H22 cells through gut microbiota regulation. Kunming mice were used as experimental subjects, and S180 and H22 tumor strains were inoculated in the left armpit of mice to establish sarcoma S180 and hepatoma H22 tumor bearing mice models. The tumor weight, tumor suppression rate, spleen and thymus weight and index, antioxidant effect,

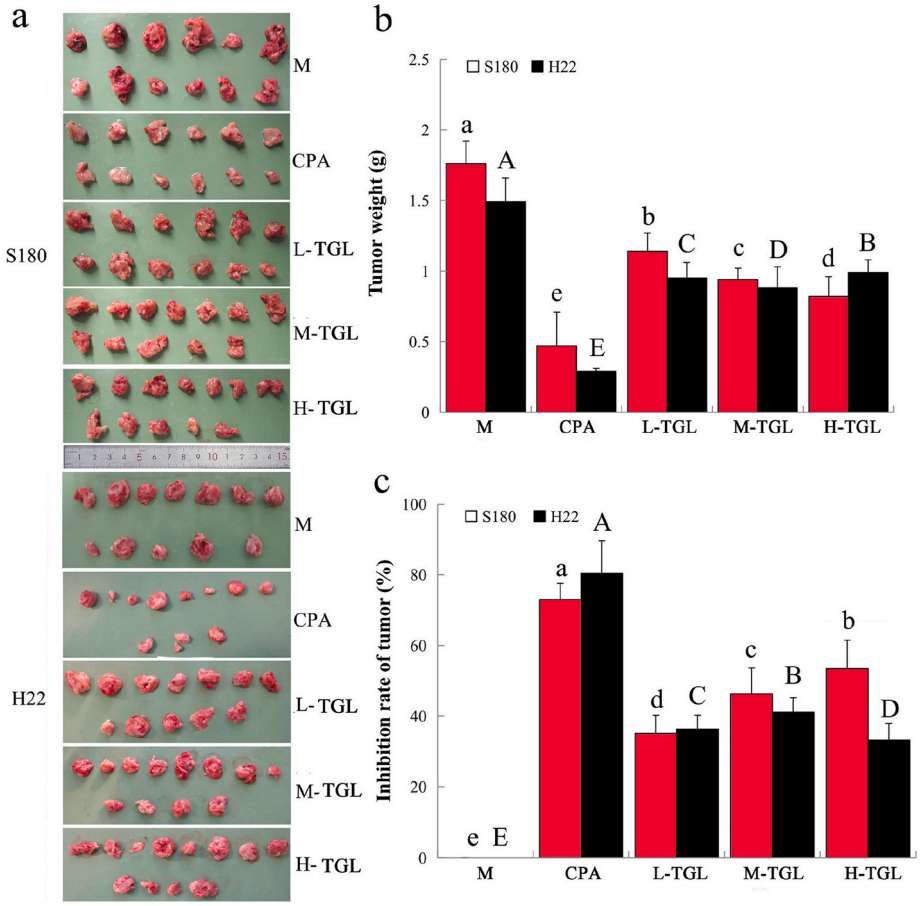

Fig. 1. Inhibition rate of cancer cell under taking TGL in Kunming mice. (a) The tumor of mice bearing S180 and H22 cells. (b) Tumor weight. (c) Tumor inhibition rate. n = 12. The different lowercase and uppercase letters means significant difference between S180 and H22 cells respectively, $p < 0.05$.

Bcl-2 and Bax gene/protein expression in tissues, and gut microbiota were measured to evaluate the anti-tumor effect of TGL. The results obtained provide latent insights into gut microbiota and oxidative stress related mechanisms underlying the antitumor effects of triterpenoids. It lays the theoretical foundation for the development of TGL functional factors with anti-tumor activity.

2. Results

2.1. Effect of TGL on tumor growth

All mice showed no adverse reactions during tumor formation, the body weight, hair color, mental state and mood of the mice were normal. With the increasing tumor volume, the activity and mental state of the mice decreased, with less exercise and loss of body weight. The tumor volume of mice in each group examined in the present study is shown that TGL has growth inhibitory effect on transplanted tumors in Fig. 1a. The change in tumor weight in mice was consistent with the change in tumor volume (Fig. 1b). As shown in Fig. 1b, TGL treatment inhibited tumor growth (H-TGL and M-TGL groups exhibited more effective reduction in the tumor weight in S180 and H22 tumor bearing mice, respectively), when compared with the model group. Each dose of TGL had an inhibitory effect on the transplanted S180 and H22 tumor bearing mice, which was significantly different from the M group ($p < 0.05$). The S180 tumor bearing mice in the H-TGL and M-TGL groups presented more than 40% tumor inhibition rates, and the CPA group showed significant tumor inhibition ($p < 0.05$) with inhibition rates higher than 70% (Fig. 1c).

2.2. Effect of TGL on spleen and thymus

The spleen and thymus are the main immune organs in the animal body, and the spleen and thymus index can reflect the body's immune capacity. The spleen and thymus volume of mice in each group examined in the present study is shown in Fig. 2a. The changes in spleen and thymus indices in mice were consistent with that in spleen and thymus volumes (Fig. 2b and c). In addition, when compared with the model group, the spleen and thymus indices of S180 and H22 tumor bearing mice in the L-TGL treatment group were significantly reduced ($p < 0.05$). However, the S180 tumor bearing mice in the H-TGL treatment group presented a relieving effect and the H22 tumor bearing mice in the M-TGL treatment group showed an alleviating effect. It can be seen that TGL has certain

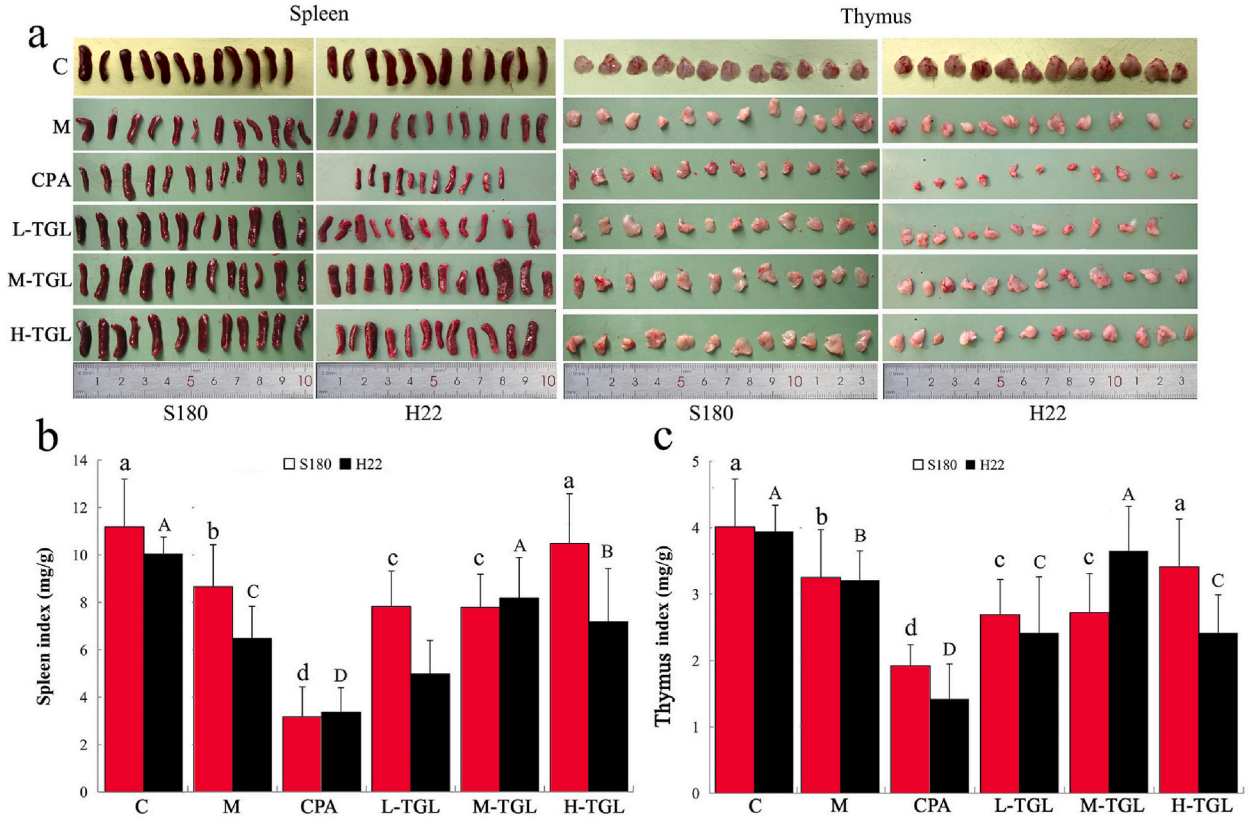

Fig. 2. Effect of TGL on immune organ and organ index in mice. (a) Spleen and thymus of mice bearing S180 and H22 cells. (b) Spleen index. (c) Thymus index. n = 12. The different lowercase and uppercase letters means significant difference between S180 and H22 cells respectively, $p < 0.05$.

effect on improving immune function within a certain dose range.

2.3. Effects of TGL on lipid peroxidation

As shown in Fig. 3a–c, when compared with the model group, TGL treatment could significantly increase the activity of SOD and CAT in the serum of S180 and H22 tumor bearing mice to a certain extent, and simultaneously decrease the serum MDA content ($p < 0.05$). The SOD and CAT contents in S180 tumor bearing mice in H-TGL group and H22 tumor bearing mice in M-TGL group were higher than those noted in other treatment groups. However, the MDA contents in S180 tumor bearing mice in H-TGL group and H22 tumor bearing mice in M-TGL group were lower than those observed in the other treatment groups. In the M-TGL group, the SOD and MDA indices in the serum of S180 and H22 tumor bearing mice and the CAT index in S180 tumor bearing mice were the highest. In conclusion, TGL has some effect on regulating antioxidant function in mice.

2.4. Effects of TGL on the expression of Bax and Bcl-2 proteins

TGL treatment downregulated the expression of Bcl-2 anti-apoptotic protein, but upregulated the expression of Bax apoptotic protein in S180 tumor bearing mice and H22 tumor bearing mice (Fig. 4a). In particular, the H-TGL group presented the best effect in restoring the expression of Bcl-2 and Bax signaling pathways in S180 tumor bearing mice with high significant difference (Fig. 4a, $p < 0.05$). With regard to the H22 tumor bearing mice, the M-TGL group showed the best effect in restoring the expression of Bcl-2 and Bax signaling pathways with high significant difference (Fig. 4b, $p < 0.05$). Furthermore, TGL treatment downregulated the expression of Bcl-2, but upregulated the expression of Bax in gut of tumor bearing mice (Fig. 4b).

2.5. Effect of TGL on microbiota diversity in tumor-bearing mice

The microbiota in the colon of tumor-bearing mice were analyzed by high-throughput sequencing spanning the 16S rDNA V3–V4 hypervariable region to show the effects of TGL on the gut microbiota in mice. Chao1 and ACE indexs were positively correlated with the gut microbiota richness in different groups. The Shannon value was positively related to diversity, while the Simpson value

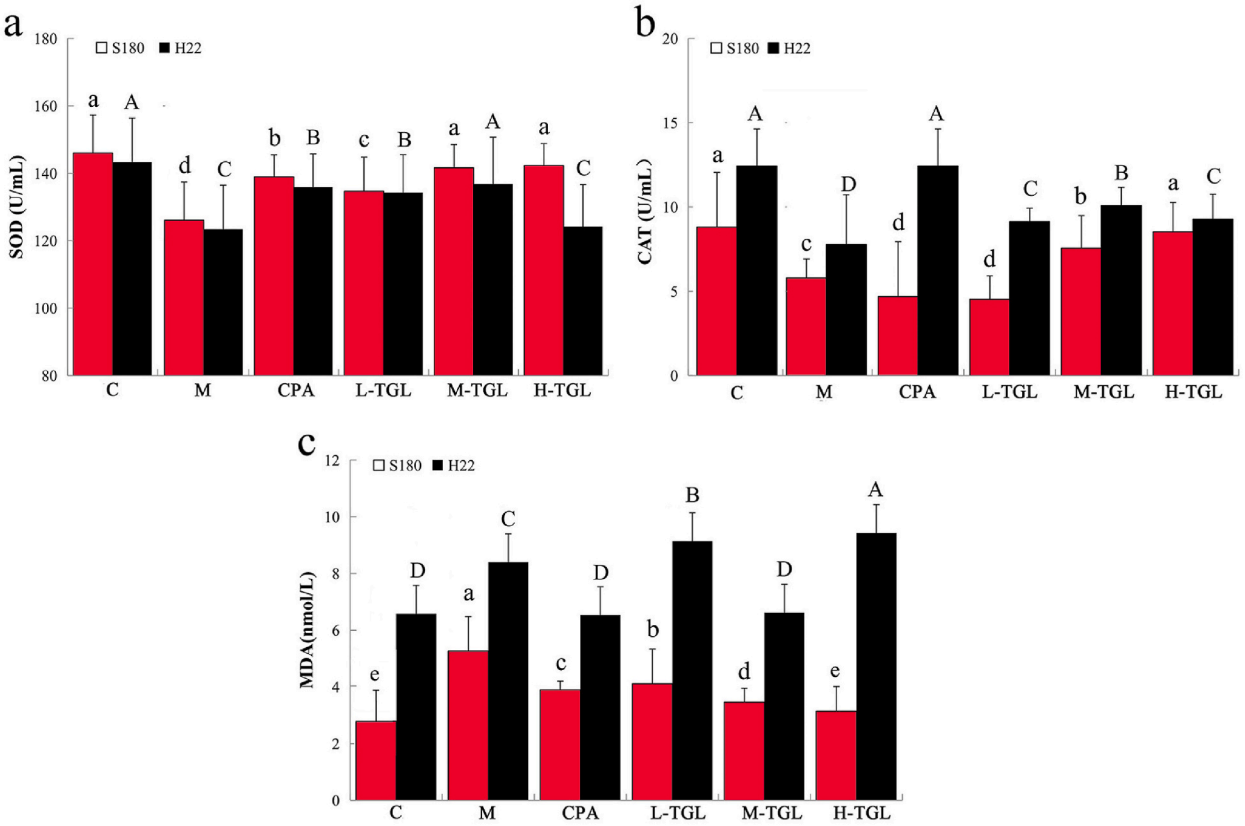

Fig. 3. Effect of TGL on the antioxidant components in the serum of mice bearing S180 and H22 cells. (a) SOD (mmol/L). (b) CAT (mmol/L). (c) MDA (mmol/L). n = 12. The different lowercase and uppercase letters means significant difference between S180 and H22 cells respectively, $p < 0.05$.

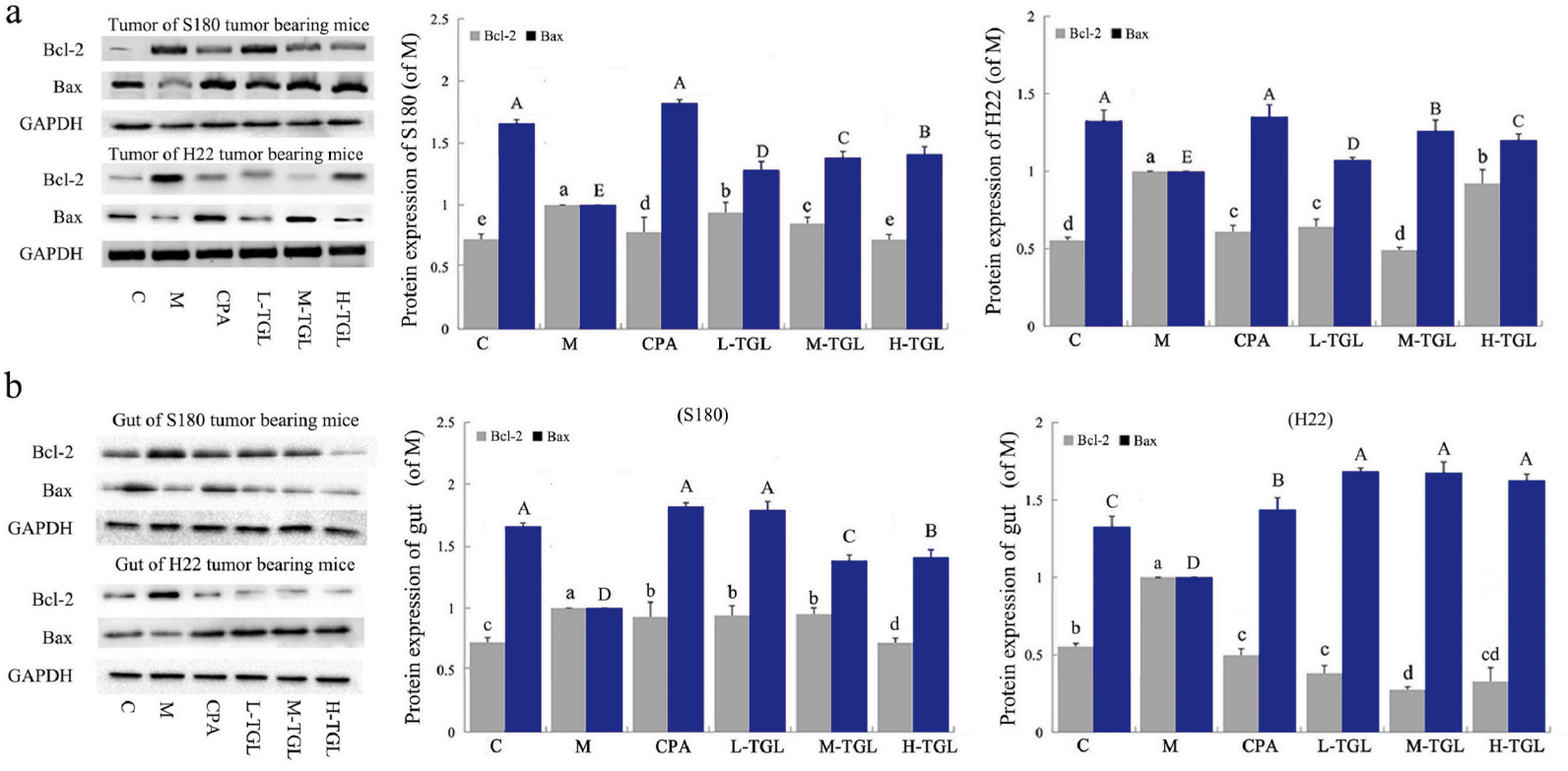

Fig. 4. Expression of Bcl-2 and Bax protein in S180 and H22 tumor and gut by TGL treatment. (a) Expression of Bcl-2 and Bax protein in S180 and H22 tumor. (b) Expression of Bcl-2 and Bax protein in gut. n = 12. The different lowercase and uppercase letters means significant difference between Bcl-2 and Bax protein expression respectively, $p < 0.05$. Original images of western blot were shown in Fig. S1.

presented the reverse trend (Table 1). The OTUs, Shannon, Chao1 and ACE indexs (community richness) were higher in TGL treatment groups, when compared with those in the M group, except for the Simpson index, indicating that TGL treatment produced higher microbial abundance and diversity in S180 and H22 tumor bearing mice.

2.6. TGL modulates the structure of gut microbiota

When compared with the CPA group, the mice S180 sarcoma M group exhibited increased relative abundance of *Bacteroides*, *Aestuariispira*, and *Acetatifactor*, and decreased relative abundance of *Barnesiella*, *Alistopes*, and *Lactobacillus* (Fig. 5a). However, TGL treatment significantly reversed this trend ($p < 0.05$) and substantially promoted the relative abundance of *Lactobacillus* ($p < 0.05$). In particular, the abundance of *Alistopes* in the M-TGL group and *Lactobacillus* in the H-TGL group was significantly higher than that in the CPA treatment group, respectively ($p < 0.05$). In H22 tumor bearing mice, TGL treatment generally increased the abundance of *Escherichia/Shigella*, *Fusobacterium*, and *Klebsiella*; and decreased the abundance of *Bacteroides* and *Parabacteroides,* when compared with the model group. To assess β-diversity, 3D-PCoA was performed among samples (Fig. 5c and d). The 3D-PCoA appeared that the control group and H-TGL group gathered together and were separated from the M group, indicating the significant differences in the gut microbiota in S180 tumor bearing mice between H-TGL group and M group (Fig. 5c). As shown in Fig. 5d, the H22 tumor bearing mice in the M-TGL group was clearly separated from the model group and close to the CPA treatment group.

Fig. 6a and b shows the line chart of species classification box of S180 and H22 tumor bearing mice. The line chart of species classification box calculates the quartile of the abundance of multiple groups of samples at different levels, and compares the differences in the abundance of different samples. At the same time, a high-level box diagram was constructed according to the relationship with the high level.

3. Conclusion and discussion

In the current study, we associated Bcl-2 and Bax gene expression in issues with gut microbiota, and further investigated the effects of TGL anti-tumor effect in mice. The data analysis confirmed TGL exerted inhibitory effects on transplanted tumors in S180 and H22 tumor bearing mice. TGL may had a positive impact on spleen, thymus and the activity of SOD and CAT in the serum, and decreased the serum MDA content to exert antitumor effects. Furthermore, TGL downregulated Bcl-2 expression and upregulated Bax expression to regulate signaling pathways. TGL regulated gut microbiota structure and abundance and had a key connection with the physiological balance and immune system of mice.

The tumor inhibition rates were higher than 30% in H22 tumor bearing mice in H-TGL and L-TGL groups, while those in the M-TGL group was more than 40%. The CPA positive control group exhibited significant tumor suppression effect ($p < 0.05$), and the tumor suppression rate was higher than 70%. This finding indicated that TGL exerted a significant inhibitory effect on the axillary transplanted S180 tumor bearing mice and H22 tumor bearing mice, and has an optimal dose range. The TGL had a higher impact on S180 tumor bearing mice in the H-TGL and M-TGL groups and H22 tumor bearing mice in the M-TGL group. Therefore, TGL may have a positive effect on the immune system to exert the antitumor effect. The relative weight of the spleen and thymus are important indicators of non-specific immunity [20]. As chemotherapeutic agents, while CPA could decrease the spleen and thymus indices, TGL could restore these indices. Therefore, TGL may have a positive impact on the immune system to exert antitumor effects. Xie et al. indicated that the water-soluble polysaccharide from *Chaenomeles speciosa* slightly decreased the spleen index, when compared with that noted in the control group, while Dong showed that polysaccharide from *Castanea mollissima* Blume could inhibit the growth of S180 solid tumors *in vivo* by protecting immune organs [20,21].

The mechanism of action of many substances with antitumor effects may be related to oxidative stress with free radical generation, which eventually causes cell damage and apoptosis [2]. In the study, the activities of superoxide dismutase, catalase, and malondialdehyde in the serum was measured showed that TGL could improve lipid peroxidation caused by the increase in free radicals *in vivo* in S180 and H22 tumor bearing mice, and exert certain antioxidant effect in tumor-bearing mice. The previous results have also confirmed that TGL have a protective effect on the immune organ. Excessive free radicals can lead to abnormal metabolism of intestinal

Table 1
Sequencing data and the alpha diversity in each group of mice (n = 12).

Type	Group	OTU	Shannon	Simpson	Chao1	ACE	Coverage
S180	C	445	3.61	0.06	472.52	489.71	1.00
	M	324	3.42	0.09	358.03	377.51	1.00
	CPA	415	3.73	0.05	461.24	471.28	1.00
	L-TGL	378	3.48	0.07	418.00	437.31	1.00
	M-TGL	392	3.72	0.05	438.87	460.62	1.00
	H-TGL	375	3.52	0.06	419.75	442.32	1.00
H22	C	438	3.53	0.06	463.33	489.21	1.00
	M	344	3.19	0.09	364.52	372.25	1.00
	CPA	407	3.58	0.04	451.87	478.36	1.00
	L-TGL	381	3.23	0.07	402.35	412.85	1.00
	M-TGL	392	3.31	0.06	443.18	442.37	1.00
	H-TGL	401	3.49	0.05	417.21	466.28	1.00

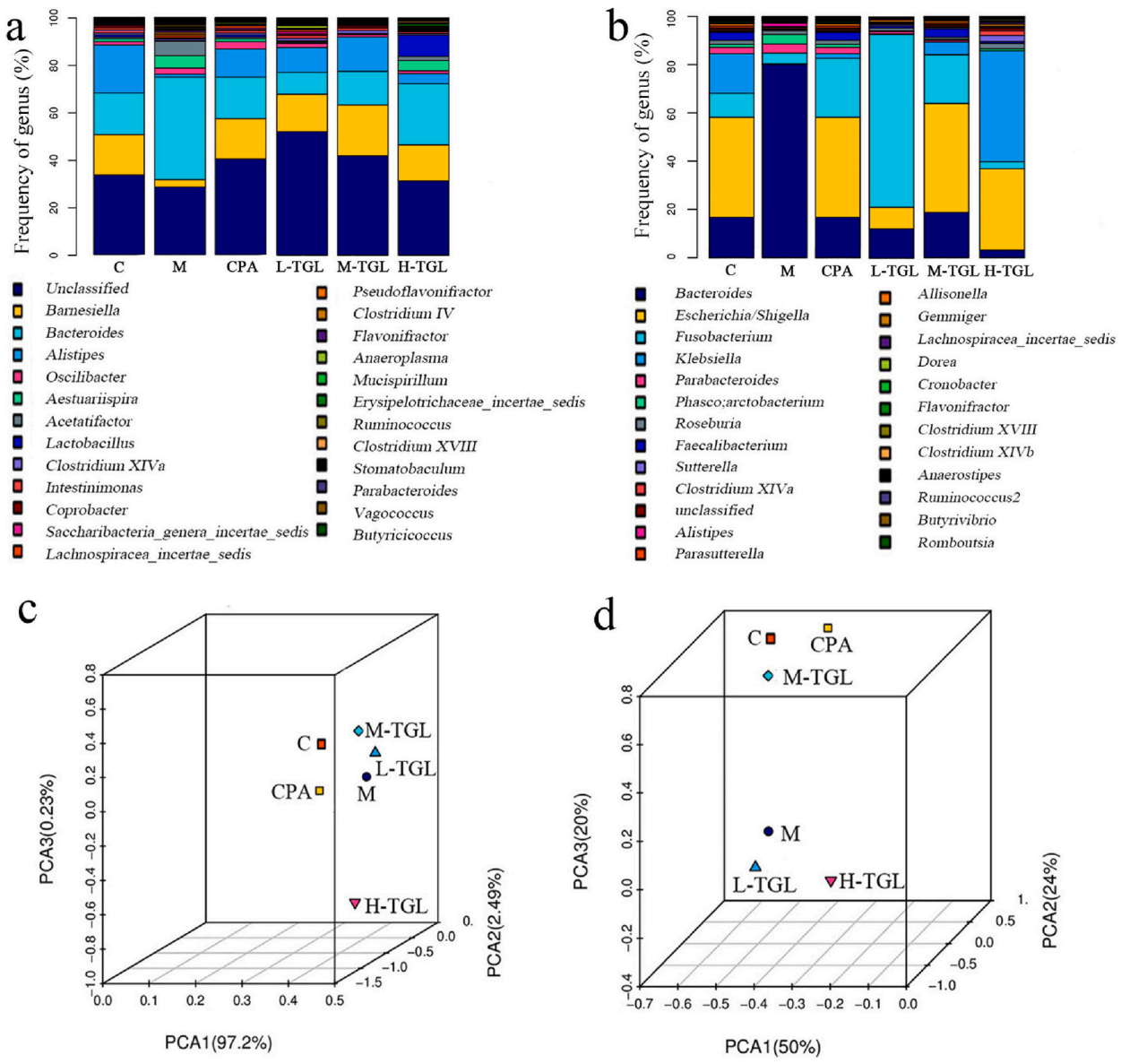

Fig. 5. Distribution of gut microbiota at different level. (a) Analysis of the composition of bacteria at the genus level of S180 tumor-bearing mice. (b) Analysis of the composition of bacteria at the genus level of H22 tumor-bearing mice. (c) 3D-PCoA of the gut microbiota of S180 tumor-bearing mice. (d) 3D-PCoA of the gut microbiota of H22 tumor-bearing mice. n = 12.

epithelial cells, impaired cell function, and inflammation [22]. In addition, oxidative stress damages the intestinal mucosa morphology and permeability, causing intestinal mucosa immune dysfunction [23]. Previous studies have shown that the loss of intestinal microbial diversity and changes in microbial composition may be related to oxidative stress levels [24]. Similar findings have also been reported by Yin et al. who indicated that pretreatment with triterpenoids from the fruits of *Sorbus pohuashanensis* could significantly increase the SOD and CAT levels and reduce the MDA content, when compared with those noted in the control group [6]. Jin et al. revealed that *Ganoderma* triterpenoids could reduce the MDA content and improve antioxidant activity [7]. Likewise, Tang et al. used *Tarphochlamys affinis* polysaccharide to treat type 2 diabetic mice and reached similar conclusions [14]. Besides, Zhang et al. also obtained similar results with polysaccharide from *Lentinus edodes*, which downregulated the Bcl-2 anti-apoptotic protein and upregulated the Bax pro-apoptotic protein in tissues [25].

These results support the notion that TGL ameliorates the decrease in gut microbiota richness resulting from the tumor. This structural change of gut microbiota may contribute to anti-tumor immunity and limit tumor expansion [26]. Xue et al. found that three soluble dietary fibers from the byproducts of mushroom *Lentinula edodes* caused the generation of unique OTUs in human gut microbiota [27]. Similarly, Yang et al. applied soy hull alcoholic extract and found that the intake of the extract could alter the

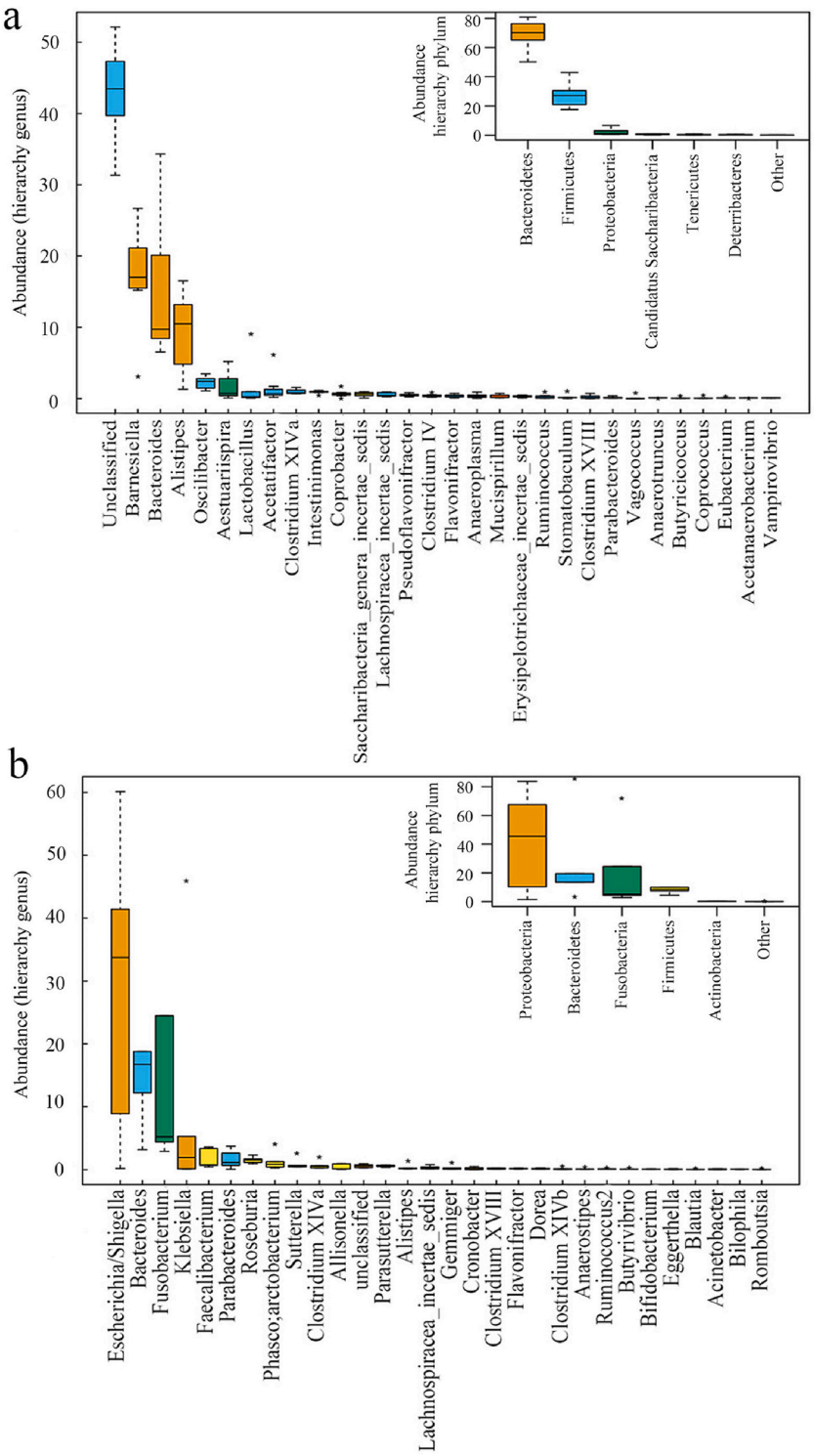

Fig. 6. Line chart of species classification box. (a) Gut microbiota of S180 tumor-bearing mice. (b) Gut microbiota of H22 tumor-bearing mice.

diversity of gut microbiota and OTUs [28]. The gut microbiota is a key factor that affects host physiology and homeostasis, including the development and function of immune system. Adolph et al. proved the importance of gut microbiota composition in cancer [29]. *Bacteroides* are important members of the colon system with the ability to digest the complex structure polysaccharides in the colon [30], while *Pasteurella* regulate immunity [18]. *Lactobacillus* spp. are beneficial to gastric and intestinal health through interaction with

the body's immune system [10]. *Fusobacterium* has been shown to have a close relationship with rectal cancer [31,32]. In a previous study, Ding et al. revealed that *Lycium barbarum* polysaccharides could modulate the composition of gut microbiota [33]. Similar to the conclusion of this experiment. Changes in gut microbiota composition affect tumor growth, partly by regulating tissue remodeling, mucosal immunity and anti-tumor immunity [16]. A study stated that the abundance of Akkermansia mucinogen was associated with human anti-PD-1 responsiveness, and the anti-tumor phenotype of melanoma patients was restored by co-administration [34]. In addition, the results of this experiment show that TGL increases the abundance of *Lactobacillus*. A study demonstrated that *Lactobacillus casei* of *Lactobacillus* has anti-tumor activity in 1984 [35]. In recent years, studies have shown that *Lactobacillus acidophilus* has anti-tumor ability and lysates of *Lactobacillus acidophilus* enhanced antitumor immunity in colon cancer model [27,36,37]. Furthermore, the irisolidonee or kakkalide isolated from *Pueraria lobata* flower significantly suppressed the fecal *Proteobacteria* population [38]. These indicate that TGL may be able to inhibit tumors by regulating intestinal microorganisms.

In conclusion, this study shows that the triterpenoids of G. lucidum has anti-tumor effects, and regulates the intestinal microorganisms. This report lays a foundation for mechanistic of natural plant extracts research on anti-tumor and prevent tumor development. The changes in multiple signaling pathways and clinical research should be investigated in the future.

4. Materials and methods

4.1. Extraction, isolation and purification of TGL

Red Ganoderma Lucidum (Species identifier: Jiajia Wang) were collected from Shifogou National Forest Park (Lanzhou City, China). Roughly crush the completely dry *G. lucidum*. Soaked powder in 95% ethanol for 3 times, and each time soaked for 7 d. Combined the three cold soaked ethanol solutions, and recycle the ethanol by rotary evaporation to obtained the alcoholie extract of TGL substance concentrate liquid (Buchi, B-490, Switzerland). The substance concentrate liquid was placed in an evaporating dish and evaporate the remaining ethanol on an 80 °C water bath to obtained the extractum of *G. lucidum* alcoholie extract. The dispersed the extractum in water was extracted 3 times with ethyl acetate, load the column with 100–200 mesh silica gel, gradient elution with chloroform-acetone and chloroform-methanol, concentrated eluent, repeated recrystallization to obtain the compound. The main compound was detected as 2α,3α,23-trihydroxy-urs-12-en-28-oic acid by gas chromatography-mass spectrometry. Its structural formula was shown in Fig. 7.

4.2. Cell culture

S180 mouse ascites sarcoma cells and H22 mouse ascites liver cancer cells were provided by Lanzhou University Institute of Pharmacology and purchased from ATCC. S180 and H22 cells were cultured in 1640 medium and Dulbecco's modified Eagle's medium (1640 and DMEM; Invitrogen; Thermo Fisher Scientific, Inc., Waltham, MA, USA) supplemented with 10% fetal bovine serum (FBS; Hyclone; GE Healthcare, Chicago, IL, USA) respectively. The cells were incubated in 95% humidified atmosphere at 37 °C in the presence of 5% CO_2 to maintain exponential cell growth.

4.3. Animal model construction

144 Kunming mice (Half male and half female, 4–6 weeks old, body weight: 20 ± 2 g), were provided by the Laboratory Animal Center of Lanzhou University and the Lanzhou Veterinary Research Institute of the Chinese Academy of Agricultural Sciences. All mice were kept in the specific pathogen free (SPF) animal laboratory, rearing conditions: room temperature (22 ± 1)°C, 12 h/12 h light/night cycle.

Under aseptic conditions, S180 (or H22) suspension cells were stained by 0.1 mL 0.2% trypan blue solution. The number of viable cells to 4×10^7 cells/ml was adjusted. The axillary skin of the left forelimb of mice was disinfected with conventional alcohol, and then 0.2 mL of diluted tumor cell suspension was injected subcutaneously. The tumor size (a) axis and small (b) axis are measured every two

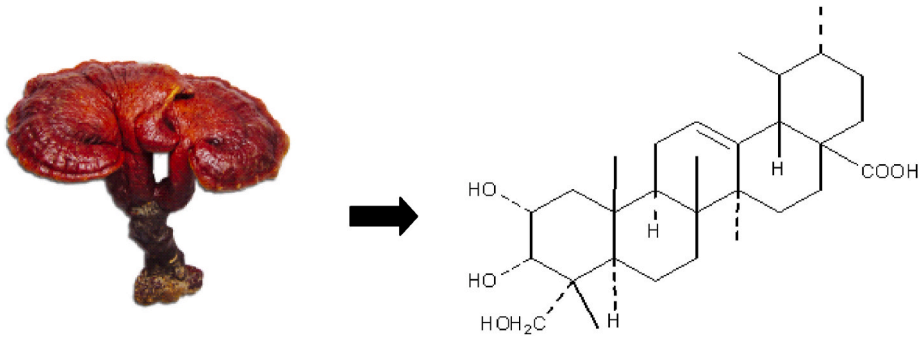

Fig. 7. Chemical structure of 2α,3α,23-trihydroxy-urs-12-en-28-oic acid of *Red Ganoderma lucidum*. (For interpretation of the references to color in this figure legend, the reader is referred to the Web version of this article.)

days to calculate the tumor volume (V). The formula was: $V = ab^2/2$ [39]. When the tumor diameter was 10 mm and the volume was 250–300 mm^3, the modeling was considered successful. Based on previous studies [40], mice were randomly allocated into Control (C) group, model (M) group, Cyclophosphamide (CPA, Shanxi Pude Pharmaceutical Co., Ltd., China) group (20 mg/kg) and TGL groups (High-dose group, H-TGL, 400 mg/kg; medium-dose group, M-TGL, 200 mg/kg; and low-dose group, L-TGL, 100 mg/kg) with 12 mice per group and provided with standard sterile food and sterile water. Gavage TGL once a day for 28 consecutive days. All tumor-bearing mice weighed once every two days, and the administration volume was 0.2 mL/10 g body weight. The mice were killed by cervical dislocation 24 h after administration on the 28th day, the corresponding organs were taken for further use. The study protocol was approved by the ethics committee of the Lanzhou Veterinary Research Institute of the Chinese Academy of Agricultural Sciences (Animal experiment permission number: 2021001).

4.4. Tumor inhibition rate

After weighing on the 29th day, S180 and H22 tumor-bearing mice were killed by the cervical spine method. Removed the tumor tissue from the mice, and remove the mice spleen and thymus to weigh. The following indicators are tested:

$$\text{Tumor inhibition rate} = (W1–W2)/W1 \times 100\% \quad (1)$$

W1: average tumor weight of the model group (g), W2: average tumor weight of the administration group (g). Throughout the experiment, observed the general condition of each group of tumor-bearing mice and the growth of the tumor.

4.5. Detection of immune organs

The mice were killed by cervical dislocation 24 h after administration on the 28th day. After the organs were rinsed with saline, the water was blotted with filter paper, weighed, and calculated according to the following formula:

$$\text{Spleen index} = \text{spleen weight (mg)/body weight (g)} \quad (2)$$

$$\text{Thymus index} = \text{thymus weight (mg)/body weight (g)} \quad (3)$$

4.6. Quantification of antioxidant components

Appropriate amounts of blood samples were collected from the tail veins of S180 and H22 tumor bearing mice. The serum was obtained by centrifugation for 1 min (2000 g, 4 °C) and was analyzed through SOD, CAT, and MDA assay kit (Nanjing Jiancheng Bioengineering Research Institute, China) based on the manufacturer's protocol, the levels of each antioxidant were measured.

4.7. Western blot

Based on previous studies [41], tumor tissues were collected and homogenized in ice-cold PBS and protease inhibitors. The total homogenate was centrifuged at high speed at 15,000 g for 20 min at 4 °C to retain the supernatant. The tumor protein concentration was detected by BCA kit (Nanjing Jiancheng Bioengineering Research Institute, China). The protein was separated on sodium dodecyl sulfate polyacrylamide gel electrophoresis (SDS-PAGE) with 10% separating gel and 4% stacking gel at 80 V for 2 h and transferred to polyvinylidene difluoride membranes for 2 h. The membranes were blocked for 1 h with PBS containing 5% BSA, and incubated with the corresponding primary monoclonal antibody IgG anti-Bcl-2, Bax and GAPDH (1:1000) (Wuhan Bode Bioengineering Co., Ltd., China) at 4 °C overnight. Subsequently, the membranes were washed with PBS with Tween for 30 min, incubated with an HRP-conjugated secondary antibody (1:5000) (Wuhan Bode Bioengineering Co., Ltd., China) for 1 h. Following 3 washes with PBS with Tween-20 for 10 min, a chemiluminescence kit (Santa Cruz Biotechnology, Inc.) was used to detect proteins. The intensity of protein was measured by AlphaView software.

4.8. DNA extraction of gut microbiota

The DNA of original gut microbiota of mice intestinal feces was extracted by QIAamp Fast DNA Stool Mini Kit (QIAGEN, Shanghai, China). Based on the manufacturer's protocol, the intestinal feces were mixed and suspended with Inhibit EX Buffer, and then the DNA was combined with QIAamp membrane. Lastly, the DNA was washed and purified from the QIAamp spin column.

4.9. 16S rDNA gene sequencing

Qubit 3.0 DNA analysis kit (Q10212, Life) was used to accurately quantify DNA and determine the amount of DNA added to the PCR reaction. The V3–V4 region of the bacteria 16S rDNA gene amplified by PCR (T100TM Thermal Cyeler, BIO-RAD), the following primers were used: 341F; 5′-CCC TAC ACG ACG CTC TTC CGA TCT G (barcode) CCT ACG GGN GGC WGC AG-3′,805R; 5′-GAC TGG AGT TCC TTG GCA CCC GAG AAT TCC AGA CTA CHV GGG TAT CTA ATC C -3′ with fusion of the Miseq sequencing platform. Prepared

PCR mixture: 10–20 ng of purified DNA, 2 × Taq master-Mix (P111-03, Vazyme) 15 μl, Bar-PCR primer F (10 μM) 1 μL, primer R (10 μM) 1 μL, and double distilled water to a final volume of 30 μL. The reaction system was as follows: an initial denaturation of 3 min at 94 °C, 5 cycles (30 s at 94 °C), 20 s at 45 °C, 30 s at 65 °C, 20 cycles (20 s at 94 °C), 20 s at 55 °C, 30 s at 72 °C, and 5 min at 72 °C. Then, a second round of amplification was performed with the introduction of Illumina bridge PCR compatible primers. This PCR system was prepared as follows: PCR products 20 ng, 2 × Taq master-Mix 15 μL, Bar-PCR primer F (10 μM) 1 μL, Primer R (10 μM), and double-distilled water to a final volume of 30 μL with PCR cycling conditions consisted of an initial denaturation of 3 min at 95 °C, 5 cycles of 20 s at 94 °C, 20 s at 55 °C, 30 s at 72 °C, and 5 min at 72 °C. PCR products were quantified and then used for Illumina MiSeq sequencing. The biological information analysis was started at operational taxonomic units (OTU) at 97% similar levels. The Ace, Chao1, Shannon, and Simpson index calculated based on the results of OTU by mothur software. Principal component analysis (PCA) and gut microbiota structure components with weighted and unweighted UniFrac analysis in R software.

4.10. Statistical analysis

The data expressed as mean ± SD (standard deviations) and differences between experimental groups were known as statistically significant if $p < 0.05$ by one-way ANOVA analysis of variance of Duncan's multiple range tests.

Ethics statement

The study protocol was approved by the ethics committee of the Lanzhou Veterinary Research Institute of the Chinese Academy of Agricultural Sciences. (Animal experiment permission number: 2021001).

Author contribution statement

Jiajia Wang: Conceived and designed the experiments; Performed the experiments; Analyzed and interpreted the data; Wrote the paper.

Junfeng Pu: Performed the experiments; Contributed reagents, materials, analysis tools or data.

Zhixian Zhang; Yanhong Wang: Performed the experiments; Analyzed and interpreted the data.

Zean Feng: Contributed reagents, materials, analysis tools or data; Wrote the paper.

Jing Han; Xiaojie Su: Analyzed and interpreted the data; Wrote the paper.

Lei Shi: Conceived and designed the experiments; Contributed reagents, materials, analysis tools or data; Wrote the paper.

Funding statement

This work was supported by the National Natural Science Foundation of Gansu Province [Grant number: 20JR10RA386].

Data availability statement

Data will be made available on request.

Declaration of competing interest

The authors declare that they have no known competing financial interests or personal relationships that could have appeared to influence the work reported in this paper

Appendix A. Supplementary data

Supplementary data to this article can be found online at https://doi.org/10.1016/j.heliyon.2023.e16682.

References

[1] E.A. Saad, H.A. Kiwan, M.M. Hassanien, Synthesis, characterization, and antitumor activity of a new iron-rifampicin complex: a novel prospective antitumor drug, J. Drug Deliv. Sci. Technol. 57 (2020), 101671.

[2] A. Abb, B. Afm, B. Das, et al., Evaluation of antitumor potential of cashew gum extracted from Anacardium occidentale Linn, Int. J. Biol. Macromol. 154 (2020) 319–328.

[3] Yang Gao, et al., Study of the extraction process and *in vivo* inhibitory effect of ganoderma triterpenes in oral mucosa cancer, Molecules 16 (7) (2011) 5315–5332.

[4] Q.Y. Kuok, C.Y. Yeh, B.C. Su, et al., The triterpenoids of Ganoderma tsugae prevent stress-induced myocardial injury in mice, Mol. Nutr. Food Res. 57 (10) (2013) 1892–1896.

[5] L. Chen, J. Pan, X. Li, et al., Endo-polysaccharide of Phellinus igniarius exhibited anti-tumor effect through enhancement of cell mediated immunity, Int. Immunopharm. 11 (2011) 255–259.

[6] Y. Yin, Y. Zhang, H. Li, Triterpenoids from fruits of Sorbus pohuashanensis inhibit acetaminophen-induced acute liver injury in mice, Biomed. Pharmacother. 109 (2019) 493–502.
[7] X. Jin, Y. Ning, Antioxidant and antitumor activities of the polysaccharide from seed cake of Camellia oleifera Abel, Int. J. Biol. Macromol. 51 (2012) 364–368.
[8] S. Haghdoost, S. Czene, I.S.S. Näslund, et al., Extracellular 8-oxo-dG as a sensitive parameter for oxidative stress *in vivo* and *in vitro*, Free Radic. Res. 39 (2005) 153–162.
[9] L. Zhang, S. Gui, J. Wang, Oral administration of green tea polyphenols (TP) improves ileal injury and intestinal flora disorder in mice with Salmonella typhimurium infection via resisting inflammation, enhancing antioxidant action and preserving tight junction, J. Funct.Foods 64 (2020), 103654.
[10] Z. Zhai, F. Zhang, R. Cao, Cecropin A alleviates inflammation through modulating the gut microbiota of C57BL/6 mice with DSS-induced IBD, Front. Microbiol. 10 (2019) 1595.
[11] S.R. Fan, G. Yu, W. Nie, et al., Antitumor activity and underlying mechanism of Sargassum fusiforme polysaccharides in CNE-bearing mice, Int. J. Biol. Macromol. 112 (2018) 516–522.
[12] H. Ji, J. Yu, A. Liu, Structural characterization of a low molecular weight polysaccharide from Grifola frondosa and its antitumor activity in H22 tumor-bearing mice, J. Funct.Foods 61 (2019), 103472.
[13] L. Cheng, L. Chen, Q. Yang, et al., Antitumor activity of Se-containing tea polysaccharides against sarcoma 180 and comparison with regular tea polysaccharides and Se-yeast, Int. J. Biol. Macromol. 120 (2018) 853–858.
[14] X. Tang, J. Huang, H. Xiong, et al., Anti-Tumor effects of the polysaccharide isolated from tarphochlamys affinis in H22 tumor-bearing mice, Cell. Physiol. Biochem. 39 (2016) 1040–1050.
[15] H. Okada, T.W. Mak, Pathways of apoptotic and non-apoptotic death in tumour cells, Nat. Rev. Cancer 4 (2004) 592–603.
[16] M.R. Rutkowski, T.L. Stephen, N. Svoronos, et al., Microbially driven TLR5-dependent signaling governs distal malignant progression through tumor-promoting inflammation, Cancer Cell 27 (2015) 27–40.
[17] M. Xue, H. Liang, X. Ji, Effects of fucoidan on gut flora and tumor prevention in 1,2-dimethylhydrazine-induced colorectal carcinogenesis, J. Nutr. Biochem. 82 (2020), 108396.
[18] R. Daille′re, M. Ve′tizou, N. Waldschmitt, et al., Enterococcus hirae and barnesiella intestinihominis facilitate cyclophosphamide-Induced therapeutic immunomodulatory effects, Immunity 45 (2016) 931–943.
[19] E.A. Vasievich, L. Huang, The suppressive tumor microenvironment: a challenge in cancer immunotherapy, Mol. Pharm. 8 (2011) 635–641.
[20] X. Dong, Y. Feng, Y. Liu, et al., A novel polysaccharide from Castanea mollissima Blume: preparation, characteristics and antitumor activities in vitro and in vivo, Carbohydr. Polym. 240 (2020), 116323.
[21] X. Xie, G. Zou, C. Li, Antitumor and immunomodulatory activities of a water-soluble polysaccharide from Chaenomeles speciosa, Carbohydr. Polym. 132 (2015) 323–329.
[22] A. Bhattacharyya, R. Chattopadhyay, S. Mitra, S.E. Crowe, Oxidative stress: an essential factor in the pathogenesis of gastrointestinal mucosal diseases, Physiol. Rev. 94 (2014) 329–354.
[23] B. Mishra, R. Jha, Oxidative stress in the poultry gut: potential challenges and interventions, Front. Vet. Sci. 6 (2019) 60.
[24] J. Halfvarson, C.J. Brislawn, R. Lamendella, et al., Dynamics of the human gut microbiome in inflammatory bowel disease, Nat. Microbiol. 2 (2017), 17004.
[25] Y. Zhang, Y. Shu, H. Wang, Induction of apoptosis in S180 tumour bearing mice by polysaccharide from Lentinus edodes via mitochondria apoptotic pathway, J. Funct.Foods 15 (2015) 151–159.
[26] Y. Li, L. Elmén, I. Segota, et al., Gut microbiota dependent anti-tumor immunity restricts melanoma growth in Rnf5-/-mice, Nat. Commun. 10 (2019) 1492.
[27] Z. Xue, Q. Ma, Y. Chen, Structure characterization of soluble dietary fiber fractions from mushroom Lentinula edodes (Berk.) Pegler and the effects on fermentation and human gut microbiota in vitro, Food Res. Int. 129 (2020), 108870.
[28] L. Yang, Y. Zhao, J. Huang, Insoluble dietary fiber from soy hulls regulates the gut microbiota *in vitro* and increases the abundanceiales and lactobacillales, J. Food Sci. Technol. 57 (2019) 152–162.
[29] T.E. Adolph, M.F. Tomczak, F. Niederreiter, et al., Paneth cells as a site of origin for intestinal inflammation, Nature 503 (2013) 272–276.
[30] N. Zeybek, R.A. Rastall, A.O. Buyukkileci, Utilization of xylan-type polysaccharides in co-culture fermentations of Bifidobacterium and Bacteroides species, Carbohydr. Polym. 236 (2020), 116076.
[31] A.D. Kostic, D. Gevers, C.S. Pedamallu, Genomic analysis identifies association of Fusobacterium with colorectal carcinoma, Genome Res. 22 (2012) 292–298.
[32] M. Castellarin, R.L. Warren, J.D. Freeman, et al., Fusobacterium nucleatum infection is prevalent in human colorectal carcinoma, Genome Res. 22 (2012) 299–306.
[33] Y. Ding, Y. Yan, Y. Peng, et al., In vitro digestion under simulated saliva, gastric and small intestinal conditions and fermentation by human gut microbiota of polysaccharides from the fruits of Lycium barbarum, Int. J. Biol. Macromol. 125 (2018) 751–760.
[34] B. Routy, E. Le Chatelier, L. Derosa, Gut microbiome influences efficacy of PD-1-based immunotherapy against epithelial tumors, Science 6371 (2018) 91–97.
[35] N. Yasutake, M. Ohwaki, T. Yokokura, Comparison of antitumor activity of Lactobacillus casei with other bacterial immunopotentiators, Med. Microbiol. Immunol. 173 (1984) 113.
[36] J. He, Z. Wu, D. Pan, et al., Effect of selenylation modification on antitumor activity of peptidoglycan from Lactobacillus acidophilus, Carbohydr. Polym. 165 (2017) 344–350.
[37] Q. Zhuo, B. Yu, J. Zhou, Lysates of Lactobacillus acidophilus combined with CTLA-4-blocking antibodies enhance antitumor immunity in a mouse colon cancer model, Sci. Rep. 9 (2019), 20128.
[38] H.M. Jang, K.T. Park, H.D. Noh, et al., Kakkalide and irisolidone alleviate 2,4,6-trinitrobenzenesulfonic acid-induced colitis in mice by inhibiting lipopolysaccharide binding to toll-like receptor-4 and proteobacteria population, Int. Immunopharm. 73 (2019) 246–253.
[39] L. Yang, Y. Liu, C. Sun, Inhibition of DNA-PKcs enhances radiosensitivity and increases ATM and ATR levels in NSCLC cells exposed to carbon ion irradiation, Oncol letters 10 (2015) 2856–2864.
[40] Q. Lin, L.N. Yang, L. Han, Effect of the soy hull polysaccharide on gut microbiota of rats with high-fat-high-sucrose diet, Food Sci. Hum. Wellness 11 (2022) 49–57.
[41] L. Yang, Q. Lin, L. Han, Soy hull dietary fiber alleviates inflammation in BALB/C mice by modulating the gut microbiota and suppressing the TLR-4/NF-κB signaling pathway, Food Funct. 11 (2020) 5965–5975.